

This Page Is Inserted by IFW Operations
and is not a part of the Official Record

BEST AVAILABLE IMAGES

Defective images within this document are accurate representations of the original documents submitted by the applicant.

Defects in the images may include (but are not limited to):

- BLACK BORDERS
- TEXT CUT OFF AT TOP, BOTTOM OR SIDES
- FADED TEXT
- ILLEGIBLE TEXT
- SKEWED/SLANTED IMAGES
- COLORED PHOTOS
- BLACK OR VERY BLACK AND WHITE DARK PHOTOS
- GRAY SCALE DOCUMENTS

IMAGES ARE BEST AVAILABLE COPY.

**As rescanning documents *will not* correct images,
please do not report the images to the
Image Problem Mailbox.**

Sebastian Flacke, MD
 John S. Allen, BA
 Jon M. Chia, MS
 James H. Wible, PhD
 M. Peri Periasamy, PhD
 Max D. Adams, PhD
 I. Kofi Adzamli, PhD
 Christine H. Lorenz, PhD

Index terms:

Contrast media, comparative studies
 Contrast media, experimental studies
 Magnetic resonance (MR), contrast media, 511.121412, 511.121413, 511.12143

Manganese
 Myocardium, infarction, 511.771

Published online before print
 10.1148/radiol.2263020151
 Radiology 2003; 226:731-738

Abbreviation:

CNR = contrast-to-noise ratio

¹ From the Center for Cardiovascular Magnetic Resonance, Department of Medicine, Cardiovascular Division, Washington University Medical School, St Louis, Mo (S.F., J.S.A., J.M.C., C.H.L.); and Imaging Division, Mallinckrodt, St Louis, Mo (J.H.W., M.P.P., M.D.A., I.K.A.). Received March 4, 2002; revision requested April 23; final revision received July 31; accepted August 14. S.F. supported by German Research Foundation grant FL-330. Address correspondence to S.F., Department of Radiology, University of Bonn, Sig-mund-Freud-Strasse 25, D-53105 Bonn, Germany (e-mail: flacke@uni-bonn.de).

Author contributions:

Guarantors of integrity of entire study, S.F., C.H.L.; study concepts and design, S.F., C.H.L.; literature research, S.F.; experimental studies, S.F., J.S.A., J.M.C.; data acquisition, S.F., J.S.A., J.M.C.; data analysis/interpretation, S.F., C.H.L., I.K.A.; statistical analysis, S.F.; manuscript preparation and editing, S.F.; manuscript definition of intellectual content, S.F., C.H.L.; manuscript revision/review and final version approval, S.F., J.H.W., M.P.P., M.D.A., I.K.A., C.H.L.

© RSNA, 2003

Characterization of Viable and Nonviable Myocardium at MR Imaging: Comparison of Gadolinium-based Extracellular and Blood Pool Contrast Materials versus Manganese-based Contrast Materials in a Rat Myocardial Infarction Model¹

PURPOSE: To determine the contrast agent behavior of gadolinium-based (extracellular and albumin-binding) and manganese-based contrast media for late-enhancement imaging of myocardial infarction.

MATERIALS AND METHODS: Coronary ligation was performed in 30 rats, and they were serially imaged with segmented inversion-recovery gradient-echo magnetic resonance (MR) imaging (repetition time msec/echo time msec/inversion time msec [fixed], 5.2/2.5/430; flip angle, 15°) during 1 hour after administration of contrast media by using a 1.5-T MR unit. Serial measurements of the longitudinal relaxation were performed by using the Look-Locker approach (repetition time msec/echo time msec, 1,000/3.5; flip angle, 10°). Detection and size of infarction were evaluated at each time point and compared with end-point histologic findings.

RESULTS: For all manganese-based media, the contrast agent cleared from the blood pool rapidly. Manganese-based contrast media allowed precise labeling of viable cardiomyocytes within 30 minutes, and the labeling persisted for at least 1 hour. Accumulation of gadoversetamide in the infarct area was apparent after 5 minutes, and the peak contrast-to-noise ratio (CNR) between infarct and myocardium was comparable to the peak CNR of manganese-based contrast agents. Extracellular gadopentetate dimeglumine provided excellent infarct detection but a small imaging window for precise sizing of the infarct if a fixed inversion time of 430 msec was used. Albumin-binding gadolinium-based contrast media provided a longer imaging window, but infarct size was overestimated because of the nonspecific distribution of the unbound gadolinium agent.

CONCLUSION: When extracellular gadolinium-based agents are used for infarct size measurement, imaging parameters and timing are important because the kinetics of both normal and irreversibly injured myocardium must be considered. Manganese-based agents are highly specific and less sensitive to timing for infarct size determination, but further studies are required to determine if they are feasible for human use.

© RSNA, 2003

Myocardial infarct size, precise delineation of transmural extension, and detection of residual viability are critical parameters for individual risk stratification in the postinfarc-

tion period (1). There is growing interest in the use of magnetic resonance (MR) imaging for infarct delineation in these circumstances. The late-enhancement method with extracellular MR imaging contrast media has been shown to provide an excellent means for differentiation of viable from nonviable myocardium (2-5). This method has the following advantage: Gadopentetate dimeglumine, an extracellular agent, accumulates in irreversibly damaged tissue, while it washes out of normal myocardium; as a result, a time window for T1-weighted MR imaging of infarction is provided.

Extracellular contrast media, such as gadopentetate dimeglumine, diffuse into the enlarged accessible space through the disrupted plasma membranes of necrotic cells, but they also diffuse into areas of associated edema, which bears a potential risk to cause overestimation of the size of the infarct (6-8). Furthermore, it has also been shown that accurate determination of infarct size by means of delayed enhancement requires specific timing after gadopentetate dimeglumine injection (9). These observations indicate that enhancement observed in myocardial infarction after administration of gadopentetate dimeglumine is a dynamic process that is dependent on the distribution volume of the contrast agent (7).

Other types of MR imaging contrast media, such as manganese-based agents, are of interest for infarct imaging since manganese is potent for T1 shortening and is taken up only in cells capable of active calcium transport, and thereby provides an analog to thallium imaging (10-12). Because manganese competes with calcium uptake, concerns about the potential for negative inotropic effects led to the evaluation of formulations of $MnCl_2$ dissolved in calcium gluconate for injection (13) and chelated manganese preparations, such as mangafodipir trisodium (Teslascan; Nycomed Amersham, Princeton, NJ), which is already approved for imaging of the liver.

A third possible approach is to use gadolinium-based media, such as MS-325 (Epix Medical, Cambridge, Mass) and MP-2269 (Mallinckrodt, St Louis, Mo), that bind to albumin in the blood pool (approximately 80% binding) (14,15). They thus have a longer residence time in the blood pool, whereas the free component distributes in a similar manner as extracellular media (16,17).

The purpose of this study was to determine the contrast agent behavior of gadolinium-based (extracellular and albumin-binding) and of manganese-based

contrast media for late-enhancement imaging of myocardial infarction and to assess the utility of these contrast media for infarct detection and infarct sizing.

MATERIALS AND METHODS

Experimental Protocol

Animal protocols were approved by the Animal Studies Committee at Washington University, St Louis, Mo. In 35 mature male Sprague-Dawley rats (Harlan Bioproducts, Indianapolis, Ind) that weighed 326 ± 20 (SD), ligation of the left anterior descending artery was performed to create myocardial infarction in the anterior and lateral wall of the left ventricle. A 3-4-mm permanent suture was placed through the left ventricle at the level of the left atrium. Five animals died during or after surgery, and 30 animals remained.

One week following surgery, rats were randomized to one of five groups ($n = 6$ in each group) and were imaged with a 1.5-T clinical imaging unit (Gyrosan NT; Philips Medical Systems, Best, the Netherlands) with a custom surface coil (3 cm in diameter). Different groups of animals were used, rather than serial imaging with each contrast agent in each animal, to study infarction at the same time point (1 week). Since infarcted areas undergo rapid changes in the first weeks, we thought this was more important than attempting to account for washout kinetics for each agent in the same animal. The animals were anesthetized by means of a nose cone with isoflurane at a 1.5%-2.0% volume mixed with O_2 at a rate of 2 L/min to minimally affect contractility and to minimize arrhythmias. Electrocardiographic leads were attached for monitoring and triggering of image acquisition. A catheter was placed into the tail vein for administration of contrast media.

MR Imaging Contrast Media

All contrast media used in this study were synthesized by a manufacturer (Mallinckrodt, St Louis, Mo). Varying doses were selected to be consistent with those in previous studies in the literature. Two gadolinium-based and three manganese-based contrast media were used: gadoversetamide (OptiMARK; Mallinckrodt) was used as a nonspecific gadolinium-based agent at a dose of 100 μ mol per kilogram of body weight, the standard clinical dose for approved extracellular MR contrast agents. MP-2269, an albumin-bind-

ing gadolinium-based blood pool agent, was injected at a dose of 30 μ mol/kg (14), which was similar to the practical dose for the analogous agent used in clinical trials (15).

The following three manganese-based media were used: $MnCl_2$ (dose, 15 μ mol/kg); a $MnCl_2$ /Ca mixture (dose, 15 μ mol/kg), with a manganese-calcium ratio of 1:8; and $Mn[EDTA\text{-bis(aminopropanediol)}]$, henceforth designated MP-680 (Mallinckrodt) (dose, 45 μ mol/kg) (18), a weakly chelated manganese complex. In comparison with the free manganese sources, a threefold higher dose of MP-680 was used in this study to permit faster contrast evolution, as was previously demonstrated for mangafodipir trisodium, an approved weak manganese complex (11,19). A bolus injection was used for the gadolinium-based media, whereas manganese-based media were injected over a period of 60 seconds to avoid potential cardiotoxic effects associated with bolus administration (20).

MR Imaging Protocol

Infarct imaging was performed at baseline and at 5, 10, 15, 20, 30, 45, and 60 minutes after injection of contrast material with electrocardiogram-triggered segmented inversion-recovery gradient-echo MR imaging (repetition time msec/echo time msec, 5.2/2.5; flip angle, 15°; pixel size, $0.7 \times 0.7 \times 2$ mm; short axis sections, 1-3) (21). For comparison between groups the inversion time was set to 430 msec, with central k-space profiles acquired first. Each section was acquired during 100 heartbeats (turbo fast-echo shots, five; number of signals acquired, 20), with a heart rate in the animals between 300 and 350 beats per minute. Gel phantoms with a known T1 ($T1 = 156 \pm 5$ msec and 612 ± 9 msec) were included as a reference.

Serial measurements of the longitudinal relaxation of myocardium and liver were performed at baseline and during longer MR imaging (1,000/3.5; flip angle, 10°; pixel size, $0.75 \times 0.75 \times 3$ mm) intervals with the Look-Locker approach starting from 20 minutes after contrast agent administration (7).

MR Image Analysis

Inversion-recovery gradient-echo images were analyzed in two ways: (a) Signal-to-noise ratio and contrast-to-noise ratio (CNR) were calculated by measuring signal intensities in regions of interest that were 5-15 mm^2 at various time

TABLE 1
Longitudinal Relaxation Times of Normal Myocardium and Liver before and after Injection of Gadolinium- and Manganese-based MR Imaging Contrast Media

Time from Injection	Longitudinal Relaxation Time (msec)				
	MnCl ₂ *	MnCl ₂ /Ca*	MP-680†	Gadoversetamide‡	MP-2269§
Myocardium					
Precontrast	872 ± 39	870 ± 25	881 ± 51	850 ± 36	867 ± 40
25 min	403 ± 11	703 ± 32	538 ± 31	697 ± 29	520 ± 17
35 min	410 ± 17	647 ± 35	490 ± 29	703 ± 31	560 ± 21
50 min	423 ± 20	623 ± 27	468 ± 23	803 ± 28	610 ± 12
65 min	420 ± 10	640 ± 20	473 ± 24	827 ± 26	650 ± 13
Liver					
Precontrast	583 ± 48	577 ± 42	585 ± 34	580 ± 26	573 ± 31
25 min	140 ± 36	203 ± 15	115 ± 31	517 ± 32	322 ± 13
35 min	157 ± 29	230 ± 20	109 ± 28	557 ± 31	347 ± 25
50 min	170 ± 17	250 ± 36	115 ± 24	570 ± 44	373 ± 16
65 min	183 ± 15	251 ± 45	125 ± 11	575 ± 27	420 ± 21

Note.—Data are the means ± SDs.

* The dose was 15 μmol/kg.

† The dose was 45 μmol/kg.

‡ The dose was 100 μmol/kg.

§ The dose was 30 μmol/kg.

points (22). Regions of interest were placed by one reader (S.F.) in the remote myocardium within the left ventricular septum, in the left ventricular cavity, in the infarct area, and in the background ventral to the rat on each image. (b) Infarct size was measured with agreement of two readers (S.F., C.H.L.) by means of manual tracing of the borders of the entire myocardium and also of the hyperintense myocardium on each section at all time points by using software (MASS; Medis, Leiden, the Netherlands). For the gadolinium-based contrast agents, the hyperintense myocardium was considered to represent the infarct, whereas for manganese-based media the infarct was considered to be the nonenhanced dark myocardium. Because the borders between hyperintense areas and nonenhanced areas were so distinct (high contrast over near signal void), we did not consider using a semiautomated image analysis scheme to further assess infarct size. Infarct size was calculated as the percentage of the left ventricular area in each section.

From the images obtained with the Look-Locker approach, signal intensity time curves were generated for sectors of remote myocardium and a region of interest of 15–20 mm² placed in the liver, and the curves were fit to the predicted longitudinal magnetization curves of these images to determine T1 (7). The speed of washout for the myocardium and for the liver was determined by fitting a single exponential curve to the

ΔR1 versus time data, where ΔR1 was calculated as $1/T1 - 1/T1_{\text{precontrast}}$.

Postmortem Measurements

Following the imaging period of approximately 90 minutes, the animals were sacrificed. The hearts were excised and sliced into 2-mm-thick sections corresponding to the sections on MR images. Hematoxylin-eosin stains of the sections from the excised hearts were digitized, and the infarct size for each section was calculated as a percentage of the left ventricular area by using image-editing software (Adobe Photoshop; Adobe Systems, Palo Alto, Calif). Infarct area and the left ventricular myocardium were manually traced on the two sides of each section, and the arithmetic mean was calculated. Results were converted from pixels squared to millimeters squared to allow section-by-section comparison of the end-point histologic findings with the corresponding MR images.

Statistical Methods

Data were presented as means ± SDs. Measurements were compared between groups by using a one-way analysis of variance and the Scheffé post hoc test. Increase of CNR compared with the baseline value was assessed with a paired-sample Student *t* test. Bland-Altman analysis was used to determine agreement between MR imaging findings and histomorphometry. All statis-

tical tests were two tailed, and a *P* value of .05 or less was considered to indicate a statistically significant difference.

RESULTS

Kinetics of Manganese- and Gadolinium-based Contrast Media

With all three manganese-based media, the T1 of normal myocardium and liver was reduced (Table 1). The peak reduction of T1 in the myocardium with MnCl₂ was observed 23 minutes after contrast material injection. With the other two media, a peak reduction of T1 at the end of the observation time of approximately 1 hour (Fig 1) occurred as a result of competition for tissue uptake from calcium (ie, from MnCl₂/Ca) or a slow dissociation of manganese (ie, from MP-680). The peak Δ(1/T1) of MnCl₂ ($1.33 \text{ sec}^{-1} \pm 0.03$) and of the triple-dosed MP-680 ($1.00 \text{ sec}^{-1} \pm 0.07$) in the normal myocardium was significantly higher than that of MnCl₂/Ca ($0.46 \text{ sec}^{-1} \pm 0.05$, *P* < .05). There was no noticeable washout of these contrast media during the 60 minutes of imaging time (estimated half-life in the myocardium, >1 hour).

At the time the first T1 measurements were determined, approximately 20 minutes after injection of the contrast agents gadoversetamide and MP-2269, the bulk of the gadolinium-based contrast agents had already washed out of the myocardium and liver, with similar kinetics for both tissues (Fig 1, Table 1). Therefore, we were unable to determine the peak T1 reduction for both agents. The half-life in myocardium in rats was 15 minutes ± 4 for gadoversetamide compared with 44 minutes ± 7 for the albumin-binding agent MP-2269.

The gel phantoms were repetitively imaged in all measurements determined with the Look-Locker approach, and the longitudinal relaxation times of the phantom were determined to be 156 msec ± 5 and 612 msec ± 9.

Contrast Agent Behavior on Late-Enhancement Images

On baseline images, there was no difference in the CNR calculated for viable myocardium and that calculated for the infarct for all contrast media (*t* = -.323, *P* = .751). The CNRs calculated during the imaging time are shown in Figures 2 and 3, and the peak CNR for all agents is included in Table 2.

For all manganese-based contrast me-

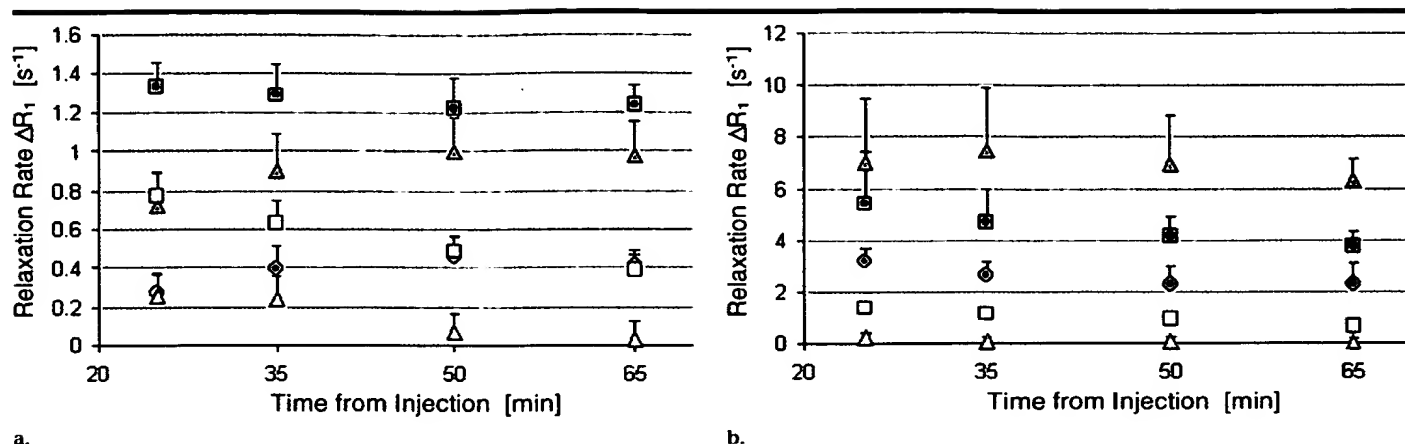


Figure 1. Graph shows T1 calculated as $1/T_1 - 1/T_{1, \text{precontrast}}$ for (a) myocardium and (b) liver at various time points for gadolinium- and manganese-based MR imaging contrast agents. All three manganese-based contrast media reduced the T1 values of normal myocardium and liver. The peak reduction of T1 in the myocardium for MnCl₂ (■) was observed 23 minutes after contrast agent injection, whereas the slower manganese release of MnCl₂/Ca (●) and MP-680 (▲) resulted in peak reduction of T1 at the end of the observation time. At the time the first T1 measurements were performed, approximately 20 minutes after injection of the contrast agents gadoversetamide (Δ) and MP-2269 (□), the bulk of the gadolinium-based agents had already washed out of the myocardium and liver, with similar kinetics for both tissues.

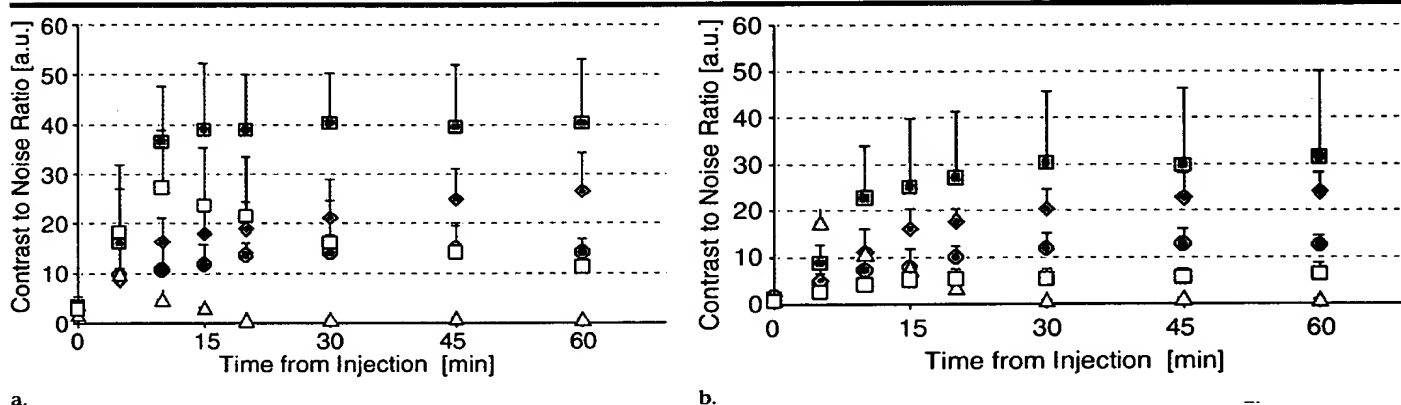


Figure 2. Graph shows CNR between (a) viable myocardium and blood and between (b) normal myocardium and infarct on inversion-recovery late-enhancement images with a fixed inversion time of 430 msec for the five groups of animals. For all manganese-based media, the contrast agent cleared from the blood pool rapidly. CNR ratios between viable myocardium and infarct were observed to have plateaued for MnCl₂ (■) approximately 30 minutes after injection and for MP-680 (◆) and MnCl₂/Ca (●) approximately 1 hour after injection. Gadoversetamide (Δ), the extracellular agent, washed out of the blood rapidly, whereas MP-2269 (□) persisted in the blood pool for the duration of the imaging. Accumulation of gadoversetamide in the infarct area was apparent after 5 minutes, which led to a peak CNR between infarct and myocardium comparable with the peak CNR of manganese-based agents.

dia, the contrast agent cleared from the blood pool rapidly. Uptake of the contrast media in myocardium was apparent at 5 minutes with MnCl₂ and MP-680 and at 10 minutes with MnCl₂/Ca, and a significant improvement of CNR was calculated for myocardium and blood, compared with the baseline CNR ($P < .05$) (Fig 3). A significant increase in CNR for normal myocardium and an infarct was observed at 5 minutes with MnCl₂, at 15 minutes with MP-680, and at 20 minutes with MnCl₂/Ca ($P < .05$), compared with the baseline CNR. CNRs for viable myocardium and an infarct

were observed to have plateaued with MnCl₂ approximately 30 minutes after contrast agent injection, whereas CNRs with MP-680 and MnCl₂/Ca showed a persistent signal intensity increase in viable myocardium throughout the imaging time, and the CNR with MnCl₂/Ca plateaued approximately 1 hour after contrast agent injection (Fig 2b).

Gadoversetamide, the extracellular agent, washed out of the blood rapidly, while MP-2269 persisted in the blood pool for the duration of the imaging. Accumulation of gadoversetamide in the infarct area was apparent after 5 minutes, and the

peak CNR between infarct and myocardium was comparable with the peak CNR of manganese-based agents (Table 2). At 30 minutes, the agent had already largely washed out of the infarcted area (Fig 3). Compared with the baseline value, a significantly increased ($P < .05$) and relatively constant CNR between viable myocardium and an infarct was observed for the blood pool agent MP-2269 from the 15-minute time point throughout the remainder of the experiment. Since the blood pool also remained enhanced, there was relatively poor contrast between the infarct and the blood pool (Fig 3).

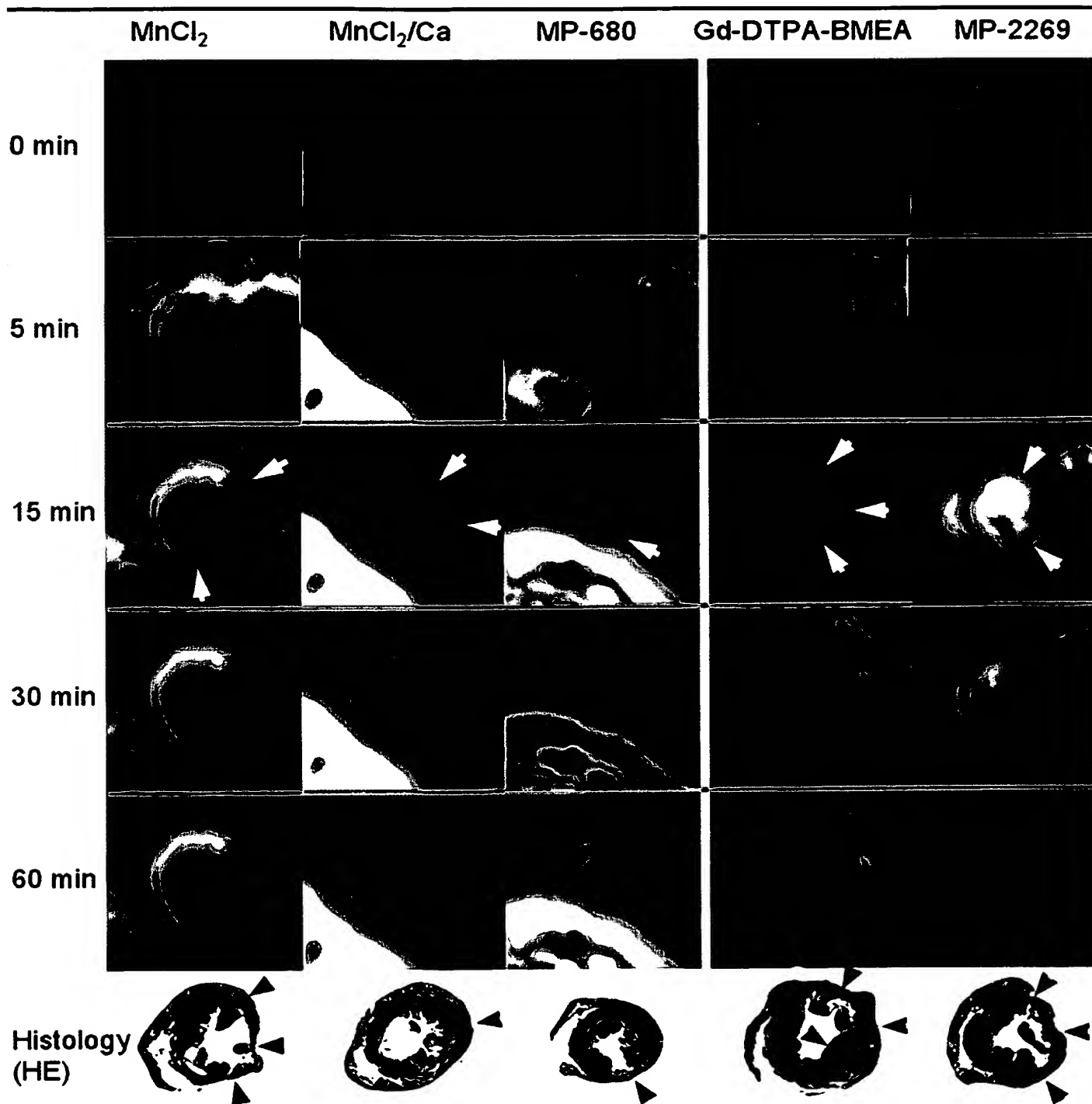


Figure 3. Late-enhancement MR images (5.2/2.5; flip angle, 15°) obtained with various contrast agents. Sample images at various time points from injection of the contrast media from each group of animals are displayed in columns. In the three columns at left, images obtained with the three manganese-based contrast agents show the viable myocardium as bright, whereas the infarct has no contrast enhancement. In the two columns at right, images obtained with both gadolinium-based contrast agents show the infarct as bright. At 15 minutes after injection, the infarcted myocardium (arrows) can be seen in all groups. Specimens of the corresponding histologic sections stained with hematoxylin-eosin are displayed in the last row. The infarct can be seen at low magnification (×5) due to the wall thinning at the poorly stained region (arrowheads). *Gd-DTPA BMEA* = gadoversetamide.

Infarct Delineation with Manganese- and Gadolinium-based Contrast Media

Sample images obtained with each contrast agent are shown in Figure 3. In three animals, histologic findings indicated no myocardial infarct. In another two animals, a small infarct was limited to the apex of the heart that was not sufficiently covered by the short-axis images of this study, and 25 animals remained for analysis of infarct size. Thus, in six of 25 animals, MnCl_2 was used; in five, MP-680 was used; in five, MnCl_2/Ca was used; in four, gadoversetamide was used; and in five, MP-2269 was used. The mean infarct size was $23\% \pm 14.4$ of the left ventricular area in each section, and there was no difference in infarct size among the five groups of animals ($P = .451$). Heterogeneity in infarct size in this model was as expected (9,11). There was good agreement between histologic findings and MR imaging findings with manganese-based contrast media (Fig 4). With respect to infarct size, the observed variability for all three manganese-based contrast media was small (approximately 10%) compared with the infarct size determined by using histologic findings. Earliest detection of myocardial infarction was possible 10 minutes after injection of MnCl_2 and 15–20 minutes after injection of MP-680 and MnCl_2/Ca .

Five minutes after injection of gadoversetamide, the area of bright myocardium was approximately $24\% \pm 3$ larger than the infarct area determined by using histologic findings. At 10 minutes after injection, there was good agreement between the areas of hyperintensity on late-enhancement images and the infarct size. With continuing washout of gadoversetamide, the bright area on late-enhancement images was smaller, and this finding led to an underestimation of infarct size (Figs 3, 4).

The blood pool agent MP-2269 allowed discrimination of the infarct area 10 minutes after injection (Fig 4). The size of the infarct was overestimated (range, 8%–15%, compared with size determined with histologic findings) during the entire imaging period. Infarct delineation was complicated at the end of the imaging period because the remaining contrast agent in the blood pool led to a higher SD of the measured infarct size at MR imaging.

DISCUSSION

Findings of This Study

In this study, contrast agent behavior of three different classes of MR imaging

TABLE 2
Mean Peak CNR between Viable Myocardium and Infarct for the Five Groups of Animals on Inversion-Recovery Late-Enhancement Images

CNR Data	Contrast Agent				
	MnCl_2	MnCl_2/Ca	MP-680	Gadoversetamide	MP-2269
Time of peak CNR after injection (min)	60	45	60	5	60
Peak CNR (arbitrary unit)*	31.3 ± 18.8	12.5 ± 3.4	23.9 ± 4.3	17.5 ± 3.0	6.1 ± 2.5

* Data are the means \pm SDs.

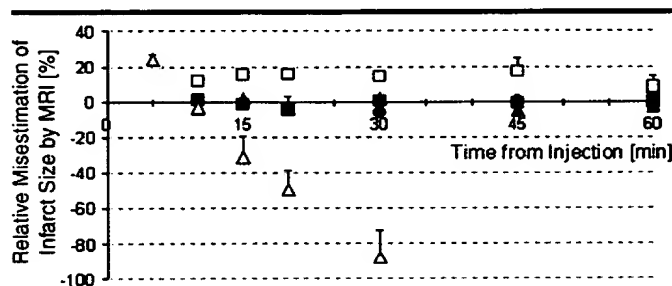


Figure 4. Graph shows estimation of infarct size by using late-enhancement MR imaging findings compared with histologic findings. The relative misestimation was calculated with a section-by-section comparison. The SD was not displayed if it was smaller than the icon size. ■ = MnCl_2 , ● = MnCl_2/Ca , ▲ = MP-680, △ = Gadoversetamide, □ = MP-2269.

contrast media was directly compared by using the late-enhancement imaging technique (2,21) at a field strength suited for human cardiac MR imaging. The major findings of this study were the following: Manganese-based contrast media with a slow manganese release allow labeling of viable cardiomyocytes with good and fairly constant contrast approximately 30 minutes after administration. Extracellular gadolinium-based contrast media provide excellent contrast between viable myocardium and an infarction, but infarct size may be overestimated early after injection. Albumin-binding gadolinium-based contrast media provide a longer imaging window for infarct delineation; however, CNRs are smaller and infarct size is overestimated likely because of the nonspecific distribution of the unbound gadolinium-based agent.

Manganese-based Agents

Manganese 52m and manganese 54 have been shown to be promising tracers for cardiac scintigraphic tomography, and the Mn^{2+} cation was also explored for cardiac imaging with MR imaging (12,23). Because manganese is a competitive antagonist at the voltage-dependent Ca^{2+} channel, cardiac toxicity is a major

concern. Reduction of myocardial contractility induced by manganese in perfused hearts can be reversed if manganese is removed from the perfusate (24). Similarly, chemical preparations with a slower release of the cation, such as mangafodipir trisodium, which is approved for clinical imaging of the liver, have a lesser effect on cardiac performance. MP-680 and MnCl_2/Ca are two formulations with an intended lower cardiac toxicity.

Wendland and co-workers (19) measured a $\Delta(1/T_1)$ for MnCl_2 of $2.5 \text{ sec}^{-1} \pm 0.3$ at a dose of $25 \mu\text{mol/kg}$ at 2 T, which is in good agreement with the peak $\Delta(1/T_1)$ of $1.33 \text{ sec}^{-1} \pm 0.03$ for MnCl_2 at a dose of $15 \mu\text{mol/kg}$ determined in this study. The $\Delta(1/T_1)$ for the weakly chelated preparation MP-680 at the three-fold dose of $45 \mu\text{mol/kg}$ was slightly lower than the values reported for mangafodipir trisodium at a dose of $50 \mu\text{mol/kg}$ (11).

The slower increase of the CNR between myocardium and blood with MP-680 reflects the longer persistence of the bound manganese in the blood pool. Both manganese-based agents, MP-680 and MnCl_2/Ca , with intended lower cardiac toxicity precisely delineated viable myocardium, but with the MnCl_2/Ca

preparation used in this study, the CNR was lower, which is likely caused by a lower availability of Mn^{2+} due to the large free calcium content.

Extracellular Gadolinium-based Contrast Media

The loss of cellular integrity and the tissue reparation that follows it has a profound influence on the distribution of extracellular MR imaging contrast media, as demonstrated by findings in recent clinical studies (2–5,25). In these studies, enhancement patterns of infarcted myocardium were associated with not only myocardial necrosis but also edema and scar formation. At peak CNR early after contrast agent injection, the extracellular agent may distribute in not only the infarct but also the surrounding area of edema, which results in an overestimation of the infarct size (8). Later after contrast agent injection, the size of enhancement matched the infarct size measured by using histologic findings. This matching of sizes may be attributed to the washout of the extracellular agent from the rim of the injured area where edema is the predominant factor of increase in distribution volume (4). With continuing observation time, further washout of the agent led to an underestimation of infarct size, which yielded a relatively short window for precise delineation of infarct size.

The time dependence of enhancement patterns observed in this study are in agreement with observations of Oshinski and co-workers (9) who found the best match between true infarct and late enhancement approximately 16 minutes after injection of gadopentetate dimeglumine in a rat infarct model. The length of the imaging window for the best match between infarct and the observed late-enhancement pattern related to not only the amount of injected contrast agent but also the circulation time. The findings of this study by using a dose of 0.1 mmol gadoversetamide in a rat model with a myocardial distribution half-life of approximately 15 minutes cannot be directly translated to human studies.

Albumin-binding Gadolinium-based Agents

The albumin-binding gadolinium-based agent MP-2269 had a longer imaging window for infarct delineation than the extracellular agent because of the longer persistence in the blood and the myocardium. The half-life in myocar-

dium of 45 minutes is in good agreement with that in previous reports in which the blood half-life in rabbits was approximately 60 minutes (14). The relatively low CNR of the infarct area and myocardium and the slight overestimation of infarct size may be attributed to an unspecific distribution of the unbound gadolinium chelate, since no conclusive findings suggest a specific binding of the agent to necrotic tissue (26). With the persistent enhancement of the blood pool, visualization of smaller subendocardial infarcts may cause problems.

Study Limitations

T1-weighted MR imaging after administration of contrast material has been used for more than a decade, but recent technical advances have dramatically improved image quality (21). In the present study, a similar sequence was used. However, for the purpose of comparison, the inversion delay was set to a fixed value for all acquisitions and was not adjusted to register postcontrast images, with the signal intensity of normal myocardium set to null. The delay was chosen to allow both sufficient suppression of normal myocardium if gadolinium-based media were used and sufficient signal recovery of normal myocardium if manganese-based media were used.

The inversion time was set to 430 msec, because the longitudinal relaxation times of myocardium after contrast agent injection were not known before this study was performed. This may have introduced a bias, because CNRs with $MnCl_2/Ca$ at the end of the observation time were measured close to the zero crossing of the myocardium, and calculation of the peak contrast was performed with incomplete suppression of viable myocardium or infarct. In future studies, the use of a phase-sensitive segmented inversion-recovery technique to avoid bounced-point ambiguity in late-enhancement images may help to overcome difficulties in interpretation of inversion-recovery images in similar settings where the precise contrast agent behavior is not known beforehand (27).

Performance of small studies in animals with a 1.5-T clinical MR imaging unit has the advantage that the techniques for imaging can be directly transferred to human studies. On the other hand, the relatively low spatial resolution of the images limits the measurement accuracy for both CNR and infarct size determination. Similarly, the resolution of the Look-Locker sequence was too low to allow measurement of T1 in

smaller infarcts. It is worth noting that the uptake time courses of the agents used may differ in humans, and intervals are likely to be scaled up. However, the relative magnitudes between the contrast of the infarct and normal contrast will be identical.

In summary, extracellular gadolinium-based contrast media provide excellent infarct detection but a small imaging window for precise infarct sizing, compared with both albumin-binding gadolinium- and manganese-based contrast media. If the safety profile of manganese-based media is acceptable for human studies, these agents may offer additional benefits since they specifically enhance viable myocardium, and the longer washout rate provides a greater window for imaging myocardial infarcts. The extent of the observed effects, however, remains to be validated in other species.

Practical application: If imaging with contrast media with a slow manganese release is performed 30 minutes or later after contrast agent injection, there is a fairly constant contrast between viable and infarcted myocardium that allows one to keep the imaging parameters constant over a longer time. Furthermore, the enhancement seen with such markers of viable myocardium is more specific, since the extent of surrounding edema, which is not known a priori, will not influence the distribution of the contrast agent.

Several unusual applications can be foreseen in which the inherent high spatial resolution of MR imaging can be combined with specific markers of viable myocardium. For example, differential contrast enhancements of manganese- and gadolinium-based contrast agents depicted in this study may be used for imaging the periinfarction zone or for excluding infarction in case of myocarditis. Additionally, manganese-based contrast agents could potentially be used in monitoring new growth of heart tissue after transplantation of stem cells.

References

1. Miller TD, Christian TF, Hopfenspirger MR, et al. Infarct size after acute myocardial infarction measured by quantitative tomographic ^{99m}Tc sestamibi imaging predicts subsequent mortality. *Circulation* 1995; 92:334–341.
2. Kim RJ, Wu E, Rafael A, et al. The use of contrast-enhanced magnetic resonance imaging to identify reversible myocardial dysfunction. *N Engl J Med* 2000; 343:1445–1453.
3. Kramer CM, Rogers WJJ, Mankad S, et al. Contrast reserve and contrast uptake pattern by magnetic resonance imaging

- and functional recovery after reperfused myocardial infarction. *J Am Coll Cardiol* 2000; 36:1835-1840.
4. Lima JA, Judd RM, Bazille A, et al. Regional heterogeneity of human myocardial infarcts demonstrated by contrast-enhanced MRI: potential mechanisms. *Circulation* 1995; 92:1117-1125.
 5. Wu KC, Zerhouni EA, Judd RM, et al. Prognostic significance of microvascular obstruction by magnetic resonance imaging in patients with acute myocardial infarction. *Circulation* 1998; 97:765-772.
 6. Arheden H, Saeed M, Higgins CB, et al. Reperfused rat myocardium subjected to various durations of ischemia: estimation of the distribution volume of contrast material with echo-planar MR imaging. *Radiology* 2000; 215:520-528.
 7. Flacke SJ, Fischer SE, Lorenz CH. Measurement of the gadopentetate dimeglumine partition coefficient in human myocardium in vivo: normal distribution and elevation in acute and chronic infarction. *Radiology* 2001; 218:703-710.
 8. Saeed M, Lund G, Wendland M, et al. Magnetic resonance characterization of the peri-infarction zone of reperfused myocardial infarction with necrosis-specific and extracellular nonspecific contrast media. *Circulation* 2001; 103:871-876.
 9. Oshinski JN, Yang Z, Jones JR, Mata JF, French BA. Imaging time after Gd-DTPA injection is critical in using delayed enhancement to determine infarct size accurately with magnetic resonance imaging. *Circulation* 2001; 104:2838-2842.
 10. Atkins HL, Som P, Fairchild RG, et al. Myocardial positron tomography with manganese-52m. *Radiology* 1979; 133:769-774.
 11. Bremerich J, Saeed M, Arheden H, et al. Normal and infarcted myocardium: differentiation with cellular uptake of manganese at MR imaging in a rat model. *Radiology* 2000; 216:524-530.
 12. Chauncey DMJ, Schelbert HR, Halpern SE, et al. Tissue distribution studies with radioactive manganese: a potential agent for myocardial imaging. *J Nucl Med* 1977; 18:933-936.
 13. Harnish P. Manganese compositions and methods for MRI. U.S. patent 5980863, 1999.
 14. Hoffman MB, Adzamlı K, Allen JS, et al. Kinetics of a novel blood pool agent (MP-2269) with persistent high relaxivity for MR angiography. *Acad Radiol* 1998; 5:206-209.
 15. Parmelee DJ, Walovitch RC, Ouellet HS, et al. Preclinical evaluation of the pharmacokinetics, biodistribution, and elimination of MS-325, a blood pool agent for magnetic resonance imaging. *Invest Radiol* 1997; 32:741-747.
 16. Simor T, Chu WJ, Johnson L, et al. In vivo MRI visualization of acute myocardial ischemia and reperfusion in ferrets by persistent action of the contrast agent Gd(BME-DTTA). *Circulation* 1995; 92:3549-3559.
 17. Schwitter L, Saeed M, Wendland MF, et al. Influence of severity of myocardial injury distribution of macromolecules: extravascular versus intravascular gadolinium-based magnetic resonance contrast agent. *J Am Coll Cardiol* 1997; 30:1086-1094.
 18. Hynes MR, Galen KP, Kuan KT, et al. Mn[EDTA-bis(APD)](code MP-680): a MR liver-specific contrast agent (abstr). In: Proceedings of the Second Meeting of the Society of Magnetic Resonance. Berkeley, Calif: Society of Magnetic Resonance, 1994; 921.
 19. Wendland MF, Saeed M, Geschwind JF, et al. Distribution of intracellular, extracellular, and intravascular contrast media for magnetic resonance imaging in hearts subjected to reperfused myocardial infarction. *Acad Radiol* 1996; 3:402-404.
 20. Wolf GL, Baum L. Cardiovascular toxicity and tissue proton T1 response to manganese injection in the dog and rabbit. *AJR Am J Roentgenol* 1983; 141:193-197.
 21. Simonetti OP, Kim RJ, Fieno DS, et al. An improved MR imaging technique for the visualization of myocardial infarction. *Radiology* 2001; 218:215-223.
 22. Henkelman RM. Measurement of signal intensities in the presence of noise in MR images. *Med Phys* 1985; 12:232-233.
 23. Maynard LS, Cotzias GC. The partition of manganese among organs and intracellular organelles in the rat. *J Biol Chem* 1955; 214:489-495.
 24. Brurok H, Ardenkjaer-Larsen JH, Hansson G, et al. Manganese dipyridoxyl diphosphate: MRI contrast agent with antioxidative and cardioprotective properties? *Biochem Biophys Res Commun* 1999; 254:768-772.
 25. Wu E, Judd RM, Vargas JD, et al. Visualization of presence, location, and transmural extent of healed Q-wave and non-Q-wave myocardial infarction. *Lancet* 2001; 357:21-28.
 26. Ni Y, Adzamlı K, Miao Y, et al. MRI contrast enhancement of necrosis by MP-2269 and gadophrin-2 in a rat model of liver infarction. *Invest Radiol* 2001; 36:97-103.
 27. Kellman P, Arai AE, McVeigh ER, et al. Phase-sensitive inversion recovery for detecting myocardial infarction using gadolinium-delayed hyperenhancement. *Magn Reson Med* 2002; 47:372-383.